

Decarboxylative Cross-Coupling Enabled by Fe and Ni Metallaphotoredox Catalysis

Reem Nsouli, Sneha Nayak‡, Venkadesh Balakrishnan‡, Jung-Ying Lin‡, Benjamin K. Chi, Hannah G. Ford, Andrew V. Tran, Ilia A. Guzei, John Bacsá, Nicholas R. Armada, Fedor Zenov, Daniel J. Weix*, Laura K. G. Ackerman-Biegasiewicz*

ABSTRACT: Decarboxylative cross-coupling of carboxylic acids and aryl halides has become a key transformation in organic synthesis to form C(sp²)–C(sp³) bonds. In this report, a base metal pairing between Fe and Ni has been developed with complementary reactivity to the well-established Ir and Ni metallaphotoredox reactions. Utilizing an inexpensive FeCl₃ co-catalyst along with a pyridine carboxamide Ni catalyst, a range of aryl iodides can be preferentially coupled to carboxylic acids over boronic acid esters, triflates, chlorides, and even bromides in high yields. Additionally, carboxylic acid derivatives containing heterocycles, *N*-protected amino acids, electron-rich amines, and protic functionality can be coupled in 23–96% yield with a range of sterically hindered, electron-rich, and electron-deficient aryl iodides. Preliminary catalytic and stoichiometric reactions support a mechanism in which Fe is responsible for the activation of carboxylic acid upon irradiation with light and a Ni(I)alkyl intermediate is responsible for activation of the aryl iodide coupling partner followed by reductive elimination to generate product.

The merger of photoredox catalysis with transition metal catalysis, metallaphotoredox catalysis, provides a valuable approach for the formation of C–C bonds.¹ These transformations enable the cross-coupling of a diverse array of carbon electrophiles and carbon nucleophile equivalents by relying on synergistic catalysis. Photoredox catalysts readily activate abundant, non-standard coupling partners via single-electron, photoinduced charge transfer followed by decarboxylation (of alkanolic acids),² β-scission (from alcohols),³ or hydrogen atom transfer mechanisms (from hydrocarbons).⁴ By comparison, transition metal catalysts are adept at net two-electron processes, such as coordination/activation of Lewis basic or pi-rich functionality⁵ or oxidative addition of organohalides.^{6,7} The ability to combine these distinct mechanisms of substrate activation has proven fruitful in a variety of contexts including arylations, alkylations, and acylations (Figure 1a).^{1,8}

A wide variety of transition metal bond-forming catalysts can be productive in these reactions, such as Pd, Au, Co, Cu, and Ni. However, the range of photocatalysts capable of enabling these transformations has been more limited.⁹ Typically, metallaphotoredox reactions have been reliant on precious metal catalysts, such as Ir and Ru, due to their stability, broad redox capabilities (for both oxidation and reduction steps), and well-understood reactivity.¹⁰ In 2014 Doyle and MacMillan first demonstrated the use of [4,4'-*Bis*(1,1-dimethylethyl)-2,2'-bipyridine-*N*1,*N*1']*bis*[3,5-difluoro-2-[5-(trifluoromethyl)-2-pyridinyl-*N*]phenyl-*C*]Iridium(III)hexafluorophosphate ((Ir[dF(CF₃)ppy]₂(dtbbpy))PF₆) and di-*tert*-butylbipyridine nickel ((dtbbpy)Ni) catalysts for the decarboxylative cross-coupling of alkyl carboxylic acids with aryl halides (Figure 1b).^{11,12} Since then, a growing number of researchers have extended

this concept to a wide range of C(sp²)–C(sp³) bond-forming reactions.¹ The high cost and limited availability of Ir have motivated a search for alternative photocatalysts, such as organic dyes made from more abundant elements. While promising results have been demonstrated, organic dyes often do not possess the same wide redox potential range as Ir dyes and there are limitations in facilitating both oxidation of the substrate and the reduction of the second catalyst.¹³ Alternatively, replacement of Ir and Ru with earth-abundant metals have suffered from short excited state lifetimes that are insufficient to induce bimolecular electron transfer (outer-sphere electron transfer).¹⁴ An emerging strategy for the development of earth-abundant metal photocatalysts is one where substrate coordination to the metal is followed by a ligand-to-metal charge transfer (LMCT) event, which induces bond homolysis (inner-sphere electron transfer). This distinct mechanism provides an opportunity for catalyst-controlled substrate activation as there is a direct interaction between the substrate and metal. Metal complexes of Co, Cu, Ni, V, Ce, Fe have been demonstrated to undergo photoinduced bond homolysis;¹⁵ however, only Ce has been paired with Ni for decarboxylative C–C bond formation via electrocatalysis,¹⁶ opening opportunities for chemical reaction discovery.¹⁷

Fe salts have emerged as an attractive alternative to Ir photocatalysts because they are inexpensive, abundant, environmentally benign, and can offer complementary reactivity to precious metal-based photocatalysts.^{18,19} As an effective Lewis acid, Fe holds promise for modulating the chemoselectivity and regioselectivity of a transformation via substrate-guided ligand effects (Figure 1c). Fe already has been demonstrated to overcome outer-sphere redox limitations, such as the

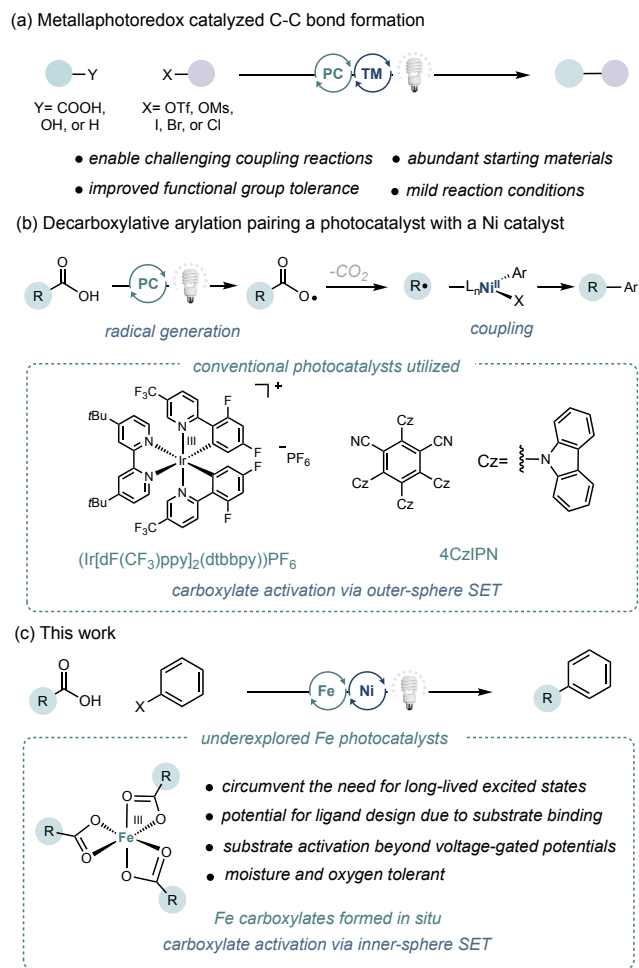


Figure 1. (a) Metallaphotoredox catalysis for C–C bond formation; (b) Metallaphotoredox strategies for decarboxylative arylation facilitated by nickel and outer-sphere photocatalysts (precious metal photocatalyst and organic dye); (c) Fe and Ni decarboxylative arylation reaction.

activation of fluoroalkyl carboxylic acids.²⁰ Additionally, Fe photocatalysts generally operate under oxidizing conditions and can tolerate air and moisture, simplifying reaction setup on the benchtop.²¹ Recently, it has been demonstrated by our group and others that catalytic amounts of Fe enable photoinduced decarboxylative functionalization with broad applications.²² These decarboxylative transformations are hypothesized to occur through Fe(III)(O(CO)R)_n (R = alkyl) complexes

that can undergo LMCT under visible light irradiation to generate a carboxylate radical and a Fe(II)(O(CO)R)_{n-1} species.^{19e} However, Fe has not been applied broadly in metallaphotoredox reactions and is yet to be developed for decarboxylative arylations.²³ We envisioned that the versatility of the Fe LMCT chemistry, when paired with the modularity of Ni, could enable a wide array of metallaphotoredox reactions.²⁴

To realize our proposed Fe and Ni metallaphotoredox system, 2-phenoxyacetic acid and 1-chloro-3-iodo-5-(trifluoromethyl)benzene were chosen as model substrates, as outlined in Table 1. These coupling partners provided a medically relevant CF₃-containing compound and could showcase the chemoselectivity of the Fe and Ni system. Based on our previous Fe-catalyzed decarboxylation studies,²¹

Table 1. Selected Optimization and Control Data for the Fe and Ni Decarboxylative Coupling.^a

entry	deviation from above	yield 1 (%)
1	none	86
2	no Fe catalyst	19
3	no Ni catalyst	0
4	no ligand	0
5	no light (60 °C)	0
6	no TBAI	73
7	with 0.5 equiv of phthalimide	90
8	Cs ₂ CO ₃ instead of <i>i</i> Pr ₂ NEt	9
9	KI instead of TBAI	72
10	TBACl instead of TBAI	31
11	427 nm instead of 390 nm	62
12	MeCN instead of 1,4-dioxane	67

^aReactions were performed on a 0.5 mmol scale. Acid (1.3 equiv), aryl halide (1 equiv), *i*Pr₂NEt (2 equiv), TBAI (1 equiv), FeCl₃ (3 mol%), Ni(NO₃)₂·6H₂O (3 mol%) and 4-*t*BuPyCam^{CN} (3 mol%) were added to 10 mL of 1,4-dioxane, and the mixture was sparged with N₂ for 5 min. The mixture was irradiated at 390 nm for 24 h. Yields were determined by ¹H NMR vs an internal standard (1,2-dibromomethane).

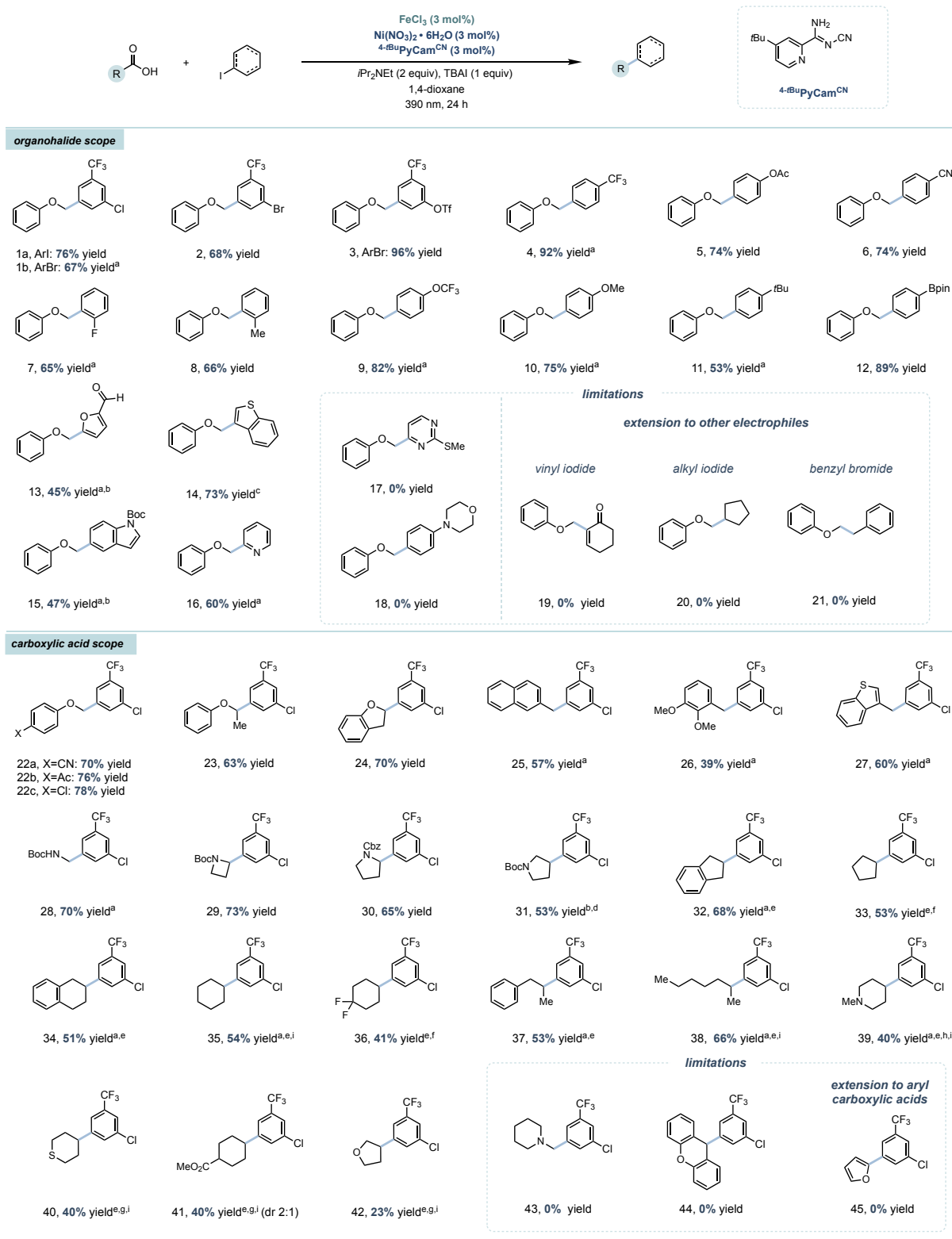


Figure 2. Organohalide and carboxylic acid scope for the Fe and Ni decarboxylative arylation reaction. Yields shown are isolated yields after purification. Reactions were performed on a 0.5 mmol scale with acid (1.3 equiv), aryl halide (1 equiv), *i*Pr₂NEt (2 equiv), TBAI (1 equiv), FeCl₃ (3 mol%), Ni(NO₃)₂·6H₂O and 4-*t*BuPyCam^{CN} (3 mol%) in 10 mL 1,4-dioxane and sparged with N₂. Reactions were irradiated at 390 nm for 24 h. ^a0.5 equivalents of phthalimide was added; ^bMeCN was used as the solvent; ^c15 mL of solvent was used; ^dNa₂CO₃ was used as base; ^eReactions run on 0.1 mmol scale with 1,4,8,11-Tetraazacyclotetradecane (cyclam) as a ligand on FeCl₃ (3 mol%); ^f15 mol% of zinc was added; ^g15 mol% of 4-ethylpyridine was added; ^h15 mol% of zinc chloride (ZnCl₂) was added. ⁱNMR yield reported by ¹H NMR vs an internal standard (1,2-dibromomethane or 1,3,5-trimethoxybenzene).

we chose FeCl₃ as the photocatalyst precursor and *N,N*-diisopropylethylamine (*i*Pr₂NEt) as the base in acetonitrile under 390 nm irradiation for the first set of experiments. Optimization commenced by assessing a variety of established ligands for Ni cross-coupling reactions. We found that 4-(*tert*-butyl)-2-(*N*-cyanocarboxamidine)pyridine (^{4-tBu}PyCam^{CN}), a ligand developed previously with Pfizer,²⁵ surfaced as the best ligand, delivering the desired product in 73% yield (Table S1). Commonly used ligands for metallaphotoredox reactions such as 4,4'-*di*-*tert*-butylbipyridine (dtbbpy) or ligands that were previously found to promote decarboxylation on Fe (2-picolinic acid and 2,2'-dipicolylamine) gave the product in only 37%, 11%, and 3% yields, respectively (Table S1). Among many possible side products, hydrodehalogenation was the most prevalent. In some cases, C-H arylation of the solvent and dimerization of the alkanolic acid were also observed. To suppress side reactivity several additives were explored, including tetrabutylammonium salts and cyclic imides (Table S7).^{26,27} We found that TBAI was superior to other salt additives (Table 1, entries 9 and 10) and the addition of 0.5 equivalents of phthalimide improved yields slightly (Table 1 entry 7). It was later shown that the impact of phthalimide was more pronounced for other substrates and was essential for accessing a general aryl iodide scope (Figure 2). Upon examining the influence of the wavelength of light, yields could be attained under blue (427 nm) light yet optimal reactivity was observed at 390 nm (Table 1, entry 11). The reaction was also amenable to a range of polar aprotic solvents and proceeded effectively in 1,4-dioxane, dimethyl carbonate, and acetonitrile (Table 1, entry 12 & Table S12). While equimolar amounts of the acid and the aryl halide resulted in high yields (Table S13) it was noted that a slight excess of acid (1.3 equiv) was beneficial potentially as a sacrificial source of electrons to reduce Ni at the start of the reaction. Control experiments for the Fe and Ni system demonstrated the need for irradiation, base, and both catalysts for practical yields to be achieved (Table 1, entries 2-5 & Table S13).

Having identified the optimal reaction conditions, we next assessed the generality of the decarboxylative arylation reaction with respect to the aryl halide coupling partner. Unlike many metallaphotoredox reactions, these reactions exhibited high selectivity for reaction at the C-I bond over C-Cl, C-Br, or C-OTf (**1-3**).²⁸ In the absence of a C-I bond, oxidative addition at C-Br also afforded the alkylated product (**1b** and **3**), but C-Cl and C-OTf bonds are unreactive under these conditions. The optimized conditions tolerated both electron-deficient and electron-rich aryl iodides with a variety of substituents at *ortho*, *meta*, and *para* positions. Aryl iodides bearing trifluoromethyl (**4**, 92% yield), acetate (**5**, 60% yield), nitrile (**6**, 74% yield), fluorine (**7**, 65% yield), and trifluoromethoxy (**9**, 68% yield) substituents all provided useful yields. Electron-rich aryl iodides (**10** and **11**), which are sometimes challenging to use in metallaphotoredox reactions, were tolerated under these conditions.^{1a,29} Reactive functional groups, such as a boronic acid pinacol ester (**12**) and an aldehyde (**13**), were also tolerated under these conditions. Moreover, this method could be utilized to functionalize several heteroaryl iodides containing furan (**13**), benzothiophene (**14**), *N*-protected indole (**15**), and pyridine (**16**). It is notable that unsubstituted pyridine does not yield Minisci chemistry side products.^{22b} Applying the standard

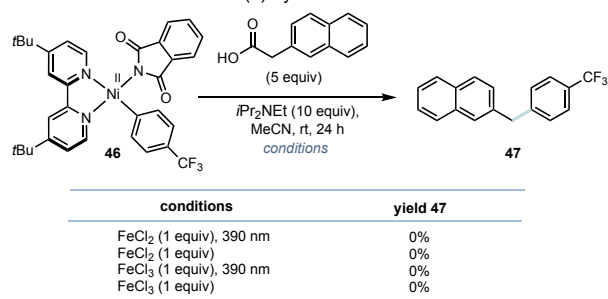
protocol to the coupling of alternative electrophiles such as vinyl iodide (**19**), alkyl iodide (**20**), or benzyl bromide (**21**) was unsuccessful without further ligand optimization.

After examining the aryl iodide scope, we examined a range of carboxylic acids under the optimized conditions (Figure 2). Prior methods using Ir as a photocatalyst have required a substantial excess (3 equiv) of carboxylic acid and exclusion of oxygen and water which has been attributed in part to the slow bimolecular SET step.³⁰ We anticipated that the use of an Fe photocatalyst might be advantageous in this context due to its facile decarboxylation via a unimolecular process.¹⁹ Initially, activated carboxylic acids were examined. Carboxylic acids with an α -heteroatom reacted under these conditions to give the expected product in excellent yields (**22-24** and **28-30**, 65-78% yield). *N*-protected α -amino acids (glycine (**28**), and proline (**30**)) and a β -amino acid (**31**) were also coupled in good yields. Benzylic acids with extended π -systems can be employed effectively (**25** and **27**) however several substrates generated unproductive alkyl dimer leading to lower or 0% yield of cross product (**26** and **44**). While the standard protocol could not be extended generally to unactivated carboxylic acids, the substitution of an inorganic base for *i*Pr₂NEt or the addition of a ligand on Fe (cyclam, to facilitate decarboxylation) proved to be successful. Arylation of cyclopentane (**33**), cyclohexane (**35**), and their derivatives (**32**, **34** and **36**) were achieved in good yields (41-68% yield). Additionally, acyclic carboxylic acids (**37** and **38**) were amenable to decarboxylation (53% and 66% yield, respectively). For several substrates the addition of Zn (**33** and **36**) or 4-ethylpyridine (**40-42**) were necessary to revive coupling activity. Finally, while electron-rich trialkyl amines are susceptible to oxidation by photocatalysts proceeding via an outer-sphere mechanism, 1-methylpiperidine-4-carboxylic acid (**39**) was tolerated and underwent successful arylation in good yield (40% yield). This result is promising and demonstrates the potential of Fe to overcome some of the challenges faced when using traditional photoredox systems. Although the reaction was applicable to a variety of sp³-carboxylic acids, the activation of sp²-carboxylic acids remains a challenge (**45**).

In order to shed light on the different reactivity between this new Fe system and more established Ir systems, we elected to study the reactivity of both potential organonickel intermediates. Many decarboxylative metallaphotoredox systems proceed through the oxidative addition of a low valent Ni(0) species into an aryl halide, yielding a Ni(II)(Ar)X intermediate which subsequently captures a radical derived from a co-catalyst. However, a conceivable alternative mechanistic pathway towards the same high valent Ni(III) species could occur through radical capture from Ni(I)X to Ni(II)(Alkyl)X. In the presence of a mild reductant this Ni(II) species can be reduced to Ni(I) followed by subsequent oxidative addition of ArI. To begin our study, we synthesized (^{tBu}bpy)Ni(Ar)(NPhth) (**46**) and (^{tBu}bpy)Ni(Alkyl)(NPhth) (**48**)^{26b,31} and studied their stoichiometric reactivity under catalytically relevant conditions (Figure 3). Yamamoto et al. noted that when X=phthalimido, these species are remarkably stable to protonation, disproportionation, and thermal decomposition.²⁶ Although reactions using dtbbpy as a ligand provided lower yields of product when compared to ^{4-tBu}PyCam^{CN}, dtbbpy offers increased synthetic

tractability and lack of ambiguous protonation state while maintaining a similar reaction profile to ^{4-tBu}PyCam^{CN}. Therefore, we elected to use dtbbpy for the following mechanistic experiments. To begin, subjecting aryl Ni precursor **46** to either FeCl₂ or FeCl₃ with or without irradiation yielded no cross product **47**, suggesting that this species is not on cycle. In contrast, product formation occurred when subjecting **48** to FeCl₂ with and without irradiation, suggesting that FeCl₂ reduces the nickel precursor **48** and that this process is not light mediated pathway. The alkylnickel(I) species formed then undergoes an oxidative addition, subsequently leading to product **47**. To further probe this reduction event, we reacted **48** with decamethylcobaltocene, a single electron reductant, to the reaction in place of FeCl₂ and this also afforded product **47**.³² As the C–C bond forming events associated with the Ni catalytic cycle are not light-mediated, we believe that the productive light-mediated reactivity in the catalytic cycle occurs through an Fe photocatalyst.

(a) stoichiometric studies with Ni(II)aryl intermediate



(b) stoichiometric studies with Ni(II)alkyl intermediate

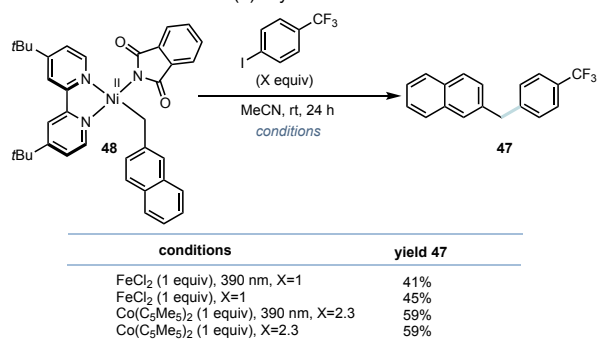


Figure 3. Stoichiometric reactions of organonickel(II) complexes. (a) Reactivity under reaction conditions with Ni(II)Aryl(NPhth) intermediate; (b) Reactivity under reaction conditions with Ni(II)Alkyl(NPhth) intermediate.

These results, in addition to the known ability of Fe(III) carboxylate species to absorb light and induce decarboxylation to form alkyl radicals and Fe(II) species,²² allows us to propose the following decarboxylative catalytic cycle (Figure 4). First, Fe carboxylate complex **50** can be generated through coordination of carboxylic acid with (L_n)Fe(III) species **49**. Under irradiation with 390 nm wavelength light, this complex then undergoes a ligand to metal charge transfer event to generate a carboxylate radical and (L_n)Fe(II) species **51**. Rapid radical decarboxylation and CO₂ extrusion leads to generation of an alkyl radical. Addition of this radical into (L_n)Ni(I)X **52** forms (L_n)Ni(II)(Alkyl)X intermediate **53**. This species then undergoes single electron reduction by (L_n)Fe(II) **51** or (L_n)Ni(I)X to form (L_n)Ni(I)(Alkyl) **54**. Reversible oxidative addition

of Ar–I forms (L_n)Ni(III)(Alkyl)(Ar)(I) **55** and reductive elimination forms cross-coupled product regenerating (L_n)Ni(I)X **52**. While this proposal is consistent with our data, additional experiments are needed to understand key aspects of the proposed cycle, such as the exact Fe species involved with and without ligand, the radical capture step by Ni, and the role of several additives that were used to expand the scope (iodide, zinc salts, and 4-ethylpyridine). Of particular interest would be an understanding of the effects of Ir and Fe mediated radical generation on the Ni catalytic cycle. These experiments are underway and will be reported in due course.

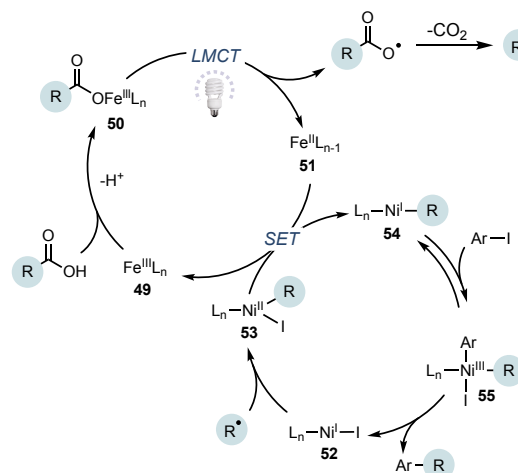


Figure 4. Proposed mechanism of Fe and Ni mediated decarboxylative arylation.

In conclusion, we report an Fe and Ni metallaphotoredox enabled decarboxylative cross coupling. The coupling of carboxylic acids and aryl iodides is both faster (24 h vs 72 h) and more tolerant to air than other reported systems.¹¹ The Ni catalyst is selective for a wide range of aryl iodides over aryl bromides, which proved challenging using an Ir and Ni system. In the absence of an aryl iodide, electron-deficient aryl bromides could be used as viable substrates. Preliminary investigation of the carboxylic acid scope demonstrated that both activated and unactivated acids, including those containing electron-rich amines, could be coupled in practical yields. Future work will be directed at understanding this new Fe and Ni catalyst system and towards developing other base metal metallaphotoredox transformations.

ASSOCIATED CONTENT

Supporting Information

The Supporting Information is available free of charge on the ACS Publications website (pdf).

AUTHOR INFORMATION

Corresponding Authors

***Laura K. G. Ackerman-Biegasiewicz**-Department of Chemistry, Emory University, Atlanta, Georgia 30322, United States; orcid.org/0000-0002-7189-1213
Email: laura.ackerman@emory.edu

***Daniel J. Weix**-Department of Chemistry, UW-Madison, Madison, WI 53706, United States; orcid.org/0000-0002-9552-3378
Email: dweix@wisc.edu

Authors

Reem Nsouli—Department of Chemistry, Emory University, Atlanta, Georgia 30322, United States; orcid.org/0000-0002-2590-1038

Sneha Nayak—Department of Chemistry, Emory University, Atlanta, Georgia 30322, United States; orcid.org/0000-0002-5571-4727

Venkadesh Balakrishnan—Department of Chemistry, Emory University, Atlanta, Georgia 30322, United States; orcid.org/0000-0002-6347-7899

Jung-Ying Lin—Department of Chemistry, Emory University, Atlanta, Georgia 30322, United States; orcid.org/0000-0001-5997-4449

Benjamin K. Chi—Department of Chemistry, UW–Madison, Madison, WI 53706, United States; orcid.org/0000-0001-5672-9827

Hannah G. Ford—Department of Chemistry, Emory University, Atlanta, Georgia 30322, United States; orcid.org/0009-0009-5937-7500

Andrew Tran—Department of Chemistry, Emory University, Atlanta, Georgia 30322, United States; orcid.org/0000-0003-3855-1353

Iliia A. Guzei—Department of Chemistry, UW–Madison, Madison, WI 53706, United States; orcid.org/0000-0003-1976-7386

John Bacsá—Department of Chemistry, Emory University, Atlanta, Georgia 30322, United States; orcid.org/0000-0001-5681-4458

Nicholas R. Armada—School of Molecular Sciences, Arizona State University, Tempe, Arizona 85281, United States

Fedor Zenov—School of Molecular Sciences, Arizona State University, Tempe, Arizona 85281, United States

Author Contributions

‡These authors contributed equally.

Funding Sources

The authors declare no competing financial interests.

ACKNOWLEDGMENT

The authors would like to acknowledge support from the Gordon and Betty Moore Foundation (GBMF11403 to LKGAB) and the NIH (R01GM097243 to DJW). The authors are grateful to Dr. Zhidao Huang (UW-Madison) for assistance with ligand synthesis.

REFERENCES

- (1) (a) Chan, A. Y.; Perry, I. B.; Bissonnette, N. B.; Buksh, B. F.; Edwards, G. A.; Frye, L. I.; Garry, O. L.; Lavagnino, M. N.; Li, B. X.; Liang, Y.; Mao, E.; Millet, A.; Oakley, J. V.; Reed, N. L.; Sakai, H. A.; Seath, C. P.; MacMillan, D. W. C. Metallaphotoredox: The Merger of Photoredox and Transition Metal Catalysis. *Chem. Rev.* **2022**, *122*, 1485–1542. (b) Skubi, K. L.; Blum, T. R.; Yoon, T. P. Dual Catalysis Strategies in Photochemical Synthesis. *Chem. Rev.* **2016**, *116*, 10035–10074.
- (2) Xuan, J.; Zhang, Z.-G.; Xiao, W.-J. Visible-Light Induced Decarboxylative Functionalization of Carboxylic Acids and their Derivatives. *Angew. Chem. Int. Ed.* **2015**, *54*, 15632–15641.
- (3) (a) Thanetchaiyakup, A.; Chin, K. F.; Dokić, M.; Tan, P. M. L.; Lin, D. J.; Mathiew, M.; Zhao, X.; Heng, J. Z. X.; Toh, D. J. X.; L, X.-W.; Ramalingam, B.; Soo, H. S. Photocatalytic deconstructive aliphatic carbon–carbon bond cleavage and functionalization of unactivated alcohols. *Chem. Catal.* **2023**, *3*, 100530. (b) Chang, L.; An, Q.; Duan, L.; Feng, K.; Zuo, Z. Alkoxy Radicals See the Light: New Paradigms of Photochemical Synthesis. *Chem. Rev.* **2022**, *122*, 2429–2486
- (c) Tsui, E.; Wang, H.; Knowles, R. R. Catalytic generation of alkoxy radicals from unfunctionalized alcohols. *Chem. Sci.* **2020**, *41*, 11124–11141. (d) Ota, E.; Wang, H.; Frye, N. L.;

Knowles, R. R. A Redox Strategy for Light-Driven, Out-of-Equilibrium Isomerizations and Application to Catalytic C–C Bond Cleavage Reactions. *J. Am. Chem. Soc.* **2019**, *141*, 1457–1462. (e) Yayla, H. G.; Wang, H.; Tarantino, K. T.; Orbe, H. S.; Knowles, R. R. Catalytic Ring-Opening of Cyclic Alcohols Enabled by PCET of Strong O–H Bonds. *J. Am. Chem. Soc.* **2016**, *138*, 10794–10797. (f) Guo, J.-J.; Hu, A.; Chen, Y.; Sun, J.; Tang, H.; Zuo, Z. Photocatalytic C–C Bond Cleavage and Amination of Cycloalkanoles by Cerium(III) Chloride Complex. *Angew. Chem. Int. Ed.* **2016**, *55*, 15319–15322.

(4) (a) Zhang, J.; Rueping, M. Metallaphotoredox catalysis for sp³ C–H functionalizations through hydrogen atom transfer (HAT). *Chem. Soc. Rev.* **2023**, *52*, 4099–4120. (b) Nagib, D. A.; Scott, M. E.; MacMillan, D. W. C. Enantioselective α -Trifluoromethylation of Aldehydes via Photoredox Organocatalysis. *J. Am. Chem. Soc.* **2009**, *131*, 10875–10877.

(5) Williams, L. J.; Bhonoah, Y.; Wilkinson, L. A.; Walton, J. W. As Nice as π : Aromatic Reactions Activated by π -Coordination to Transition Metals. *Chem. Eur. J.* **2021**, *27*, 3650–3660.

(6) (a) Halpern, J. Oxidative-Addition Reactions of Transition Metal Complexes. *Acc. Chem. Res.* **1970**, *3*, 386–392. (b) Greaves, M. E.; Humphrey, E. L. B. J.; Nelson, D. J. Reactions of nickel(0) with organochlorides, organobromides, and organiodides: mechanisms and structure/reactivity relationships. *Catal. Sci. Technol.* **2021**, *11*, 2980–2996.

(7) Marzo, L.; Pagire, S. K.; Reiser, O.; König, B. Visible-Light Photocatalysis: Does It Make a Difference in Organic Synthesis? *Angew. Chem. Int. Ed.* **2018**, *57*, 10034–10072.

(8) For metallaphotoredox examples see: (a) Lu, F.-D.; He, G.-F.; Lu, L.-Q.; Xiao, W.-J. Metallaphotoredox catalysis for multicomponent coupling reactions. *Green Chem.* **2021**, *23*, 5379–5393.

(b) Joe, C. L.; Doyle, A. G. Direct Acylation of C(sp³)–H Bonds Enabled by Nickel and Photoredox Catalysis. *Angew. Chem. Int. Ed.* **2016**, *55*, 4040–4043. (c) Yang, Q.; Zhang, L.; Ye, C.; Luo, S.; Wu, L.-Z.; Tung, C.-H. Visible-Light-Promoted Asymmetric Cross-Dehydrogenative Coupling of Tertiary Amines to Ketones by Synergistic Multiple Catalysis. *Angew. Chem. Int. Ed.* **2017**, *56*, 3694–3698.

(9) For seminal examples of metallaphotoredox catalysis see: (a) Kalyani, D.; McMurtrey, K. B.; Neufeldt, S. R.; Sanford, M. S. Room-Temperature C–H Arylation: Merger of Pd-Catalyzed C–H Functionalization and Visible-Light Photocatalysis. *J. Am. Chem. Soc.* **2011**, *133*, 18566–18569. (b) Ye, Y.; Sanford, M. S. Merging Visible-Light Photocatalysis and Transition-Metal Catalysis in the Copper-Catalyzed Trifluoromethylation of Boronic Acids with CF₃I. *J. Am. Chem. Soc.* **2012**, *134*, 9034–9037. (c) Zultanski, S. L.; Fu, G. C. Nickel-Catalyzed Carbon–Carbon Bond-Forming Reactions of Unactivated Tertiary Alkyl Halides: Suzuki Arylations. *J. Am. Chem. Soc.* **2013**, *135*, 624–627. (d) Sahoo, B.; Hopkinson, M. N.; Glorius, F. Combining Gold and Photoredox Catalysis: Visible Light-Mediated Oxy- and Aminoarylation of Alkenes. *J. Am. Chem. Soc.* **2013**, *135*, 5505–5508. (e) Tellis, J. C.; Primer, D. N.; Molander, G. A. Single-electron transmetalation in organoboron cross-coupling by photoredox/nickel dual catalysis. *Science* **2014**, *345*, 433–436. (f) Allen, L. J.; Cabrera, P. J.; Lee, M.; Sanford, M. S. N-Acyloxyphthalimides as Nitrogen Radical Precursors in the Visible Light Photocatalyzed Room Temperature C–H Amination of Arenes and Heteroarenes. *J. Am. Chem. Soc.* **2014**, *136*, 5607–5610. (g) Thullen, S. M.; Rovis, T. A Mild Hydroaminoalkylation of

- Conjugated Dienes Using a Unified Cobalt and Photoredox Catalytic System. *J. Am. Chem. Soc.* **2017**, *139*, 15504–15508.
- (10) (a) Prier, C. K.; Rankic, D. A.; MacMillan, D. W. C. Visible Light Photoredox Catalysis with Transition Metal Complexes: Applications in Organic Synthesis. *Chem. Rev.* **2013**, *113*, 5322–5363. (b) Shaw, M. H.; Twilton, J.; MacMillan, D. W. C. Photoredox Catalysis in Organic Chemistry. *J. Org. Chem.* **2016**, *81*, 6898–6926.
- (11) Zuo, Z.; Ahneman, D. T.; Chu, L.; Terrett, J. A.; Doyle, A. G.; MacMillan, D. W. C. Merging photoredox with nickel catalysis: Coupling of α -carboxyl sp^3 -carbons with aryl halides. *Science* **2014**, *345*, 437–440.
- (12) The Molander group also helped in establishing the reactivity of Ir/Ni systems using BF_3K salts as the electrophiles instead of carboxylic acids. (refer to reference 9(e)).
- (13) For the photophysical and electrochemical properties of common organic photoredox catalysts see: Romero, N. A.; Nicewicz, D. A. Organic Photoredox Catalysis. *Chem. Rev.* **2016**, *116*, 10075–10166.
- (14) (a) Wenger, O. S. Photoredox Complexes with Earth-Abundant Metals. *J. Am. Chem. Soc.* **2018**, *140*, 13522–13533. (b) Larsen, C. B.; Wenger, O. S. Photoredox Catalysis with Metal Complexes Made from Earth-Abundant Elements. *Chem. Eur. J.* **2018**, *24*, 2039–2058. (c) Hockin, B. M.; Li, C.; Robertson, N.; Zysman-Colman, E. Photoredox catalysts based on earth-abundant metal complexes. *Catal. Sci. Technol.* **2019**, *9*, 889–915.
- (15) (a) Abderrazak, Y.; Bhattacharyya, A.; Reiser, O. Visible-Light-Induced Homolysis of Earth-Abundant Metal-Substrate Complexes: A Complementary Activation Strategy in Photoredox Catalysis. *Angew. Chem. Int. Ed.* **2021**, *60*, 21100–21115. (b) Juliá, F. Ligand-to-Metal Charge Transfer (LMCT) Photochemistry at 3d-Metal Complexes: An Emerging Tool for Sustainable Organic Synthesis. *ChemCatChem* **2022**, *14*, e202200916.
- (16) (a) Chen, Y.; Wang, X.; He, X.; An, Q.; Zuo, Z. Photocatalytic Dehydroxymethylative Arylation by Synergistic Cerium and Nickel Catalysis. *J. Am. Chem. Soc.* **2021**, *143*, 4896–4902. (b) Lu, J.; Yao, Y.; Li, L.; Fu, N. Dual Transition Metal Electrocatalysis: Direct Decarboxylative Alkenylation of Aliphatic Carboxylic Acids. *J. Am. Chem. Soc.* **2023**, *145*, 26774–26782.
- (17) While this paper was in review, the coupling of alcohols with aryl halides was achieved using and Fe and Ni. (a) Zuo, L.; Sun, R.; Tao, Y.; Wang, X.; Zheng, X.; Lu, Q. Photoelectrochemical Fe/Ni cocatalyzed C-C functionalization of alcohols. *Nat. Commun.* **2023**, *15*, 5245. (b) Jaber, M.; Ozbay, Y.; Tran, G.; Amgoune, A. A unified photocatalytic strategy for the cross coupling of alcohols with aryl halides enabled by synergistic nickel and iron LMCT catalysis. *ChemRxiv*. DOI: <https://doi.org/10.26434/chemrxiv-2024-9928b>.
- (18) Based on prices listed on Sigma Aldrich, $FeCl_3$ costs \$0.052/g (\$8.43/mole) while $IrCl_3$ costs \$346/g (\$103,308.68/mole) and $Ir[dF(CF_3)ppy]_2(dtbbpy)PF_6$ costs \$998/g (\$1,119,666.18/mole). Based on prices listed on Oakwood Chemical, $FeCl_3$ costs \$0.094/g (\$15.24/mole) while $IrCl_3$ costs \$390/g (\$116,446.2/mole) and $Ir[dF(CF_3)ppy]_2(dtbbpy)PF_6$ costs \$674/g (\$756,167.34/mole).
- (19) (a) Frey, P. A.; Reed, G. H. The Ubiquity of Iron. *ACS Chem. Biol.* **2012**, *7*, 1477–1481. (b) Wenger, O. S. Is Iron the New Ruthenium? *Chem. Eur. J.* **2019**, *25*, 6043–6052. (c) Zhuo, W.-J.; Wu, X.-D.; Miao, M.; Wang, Z.-H.; Chen, L.; Shan, S.-Y.; Cao, G.-M.; Yu, D.-G. Light Runs Across Iron Catalysts in Organic Transformations. *Chem. Eur. J.* **2020**, *26*, 15052–15064. (d) Rana, S.; Biswas, J. P.; Paul, S.; Paik, A.; Maiti, D. Organic synthesis with the most abundant transition metal-iron: from rust to multitasking catalysts. *Chem. Soc. Rev.* **2021**, *50*, 243–472. (e) de Groot, L. H. M.; Ilic, A.; Schwarz, J.; Wärnmark, K. Iron Photoredox Catalysis—Past, Present, and Future. *J. Am. Chem. Soc.* **2023**, *145*, 9369–9388.
- (20) Bian, K.-J.; Lu, Y.-C.; Nemoto Jr, D.; Kao, S.-C.; Chen, X.; West, J. G. Photocatalytic hydrofluoroalkylation of alkenes with carboxylic acids. *Nat. Chem.* **2023**, *15*, 1683–1692.
- (21) Crocker, M. S.; Lin, J.-Y.; Nsouli, R.; McLaughlin, N. D.; Ackerman-Biegasiewicz, L. K. G. TGA-FTIR Guided Ligand Evaluation for Iron Photocatalyzed Decarboxylative Giese Reactions. *ChemRxiv*. DOI: 10.26434/chemrxiv-2023-fmpq9.
- (22) For Fe photocatalytic decarboxylation see: (a) Feng, G.; Wang, X.; Jin, J. Decarboxylative C–C and C–N Bond Formation by Ligand-Accelerated Iron Photocatalysis. *Eur. J. Org. Chem.* **2019**, *2019*, 6728–6732. (b) Li, Z.; Wang, X.; Xia, S.; Jin, J. Ligand-Accelerated Iron Photocatalysis Enabling Decarboxylative Alkylation of Heteroarenes. *Org. Lett.* **2019**, *21*, 4259–4265. (c) Zhang, Y.; Qian, J.; Wang, M.; Huang, Y.; Hu, P. Visible-Light-Induced Decarboxylative Fluorination of Aliphatic Carboxylic Acids Catalyzed by Iron. *Org. Lett.* **2022**, *24*, 5972–5976. (d) Kao, S.-C.; Bian, K.-J.; Chen, X.-W.; Chen, Y.; Martí, A. A.; West, J. G. Photochemical iron-catalyzed decarboxylative azidation via the merger of ligand-to-metal charge transfer and radical ligand transfer catalysis. *Chem. Catal.* **2023**, *3*, 100603. (e) Lutovsky, G. A.; Gockel, S. N.; Bundesmann, M. W.; Bagley, S. W.; Yoon, T. P. Iron-mediated modular decarboxylative cross-nucleophile coupling. *Chem.* **2023**, *9*, 1344–1346.
- (23) Xiong, N.; Li, Y.; Zeng, R. Merging Photoinduced Iron-Catalyzed Decarboxylation with Copper Catalysis for C–N and C–C Coupling. *ACS Catal.* **2023**, *13*, 1678–1685.
- (24) Diccianni, J. B.; Diao, T. Mechanism of Nickel-Catalyzed Cross-Coupling Reactions. *Trends in Chemistry* **2019**, *1*, 830–844.
- (25) Hansen, E. C.; Pedro, D. J.; Wotal, A. C.; Gower, N. J.; Nelson, J. D.; Caron, S.; Weix, D. J. New ligands for nickel catalysis from diverse pharmaceutical heterocycle libraries. *Nature* **2016**, *8*, 1126–1130.
- (26) (a) Yamamoto, T.; Kohara, T.; Yamamoto, A. Preparation and Properties of Monoalkylnickel(II) Complexes $NiR(NR^1R^2)_2$ Having Imido, Imidazolato, or Methyl Phenylcarbamato–N Ligand. *Bull. Chem. Soc. Jpn.* **1981**, *54*, 1720–1726. (b) Prieto Kullmer, C. N.; Kautzky, J. A.; Krska, S. W.; Nowak, T.; Dreher, S. D.; MacMillan, D. W. C. Accelerating reaction generality and mechanistic insight through additive mapping. *Science* **2022**, *376*, 532–539.
- (27) Piber, M.; Jensen, A. E.; Rottländer, M.; Knochel, P. New Efficient Nickel- and Palladium-Catalyzed Cross-Coupling Reactions Mediated by Tetrabutylammonium Iodide. *Org. Lett.* **1999**, *1*, 1323–2326.
- (28) (a) Sanosa, N.; Ruiz-Campos, p.; Ambrosi, D.; Sampedro, D.; Funes-Ardoiz, I. Investigating the Mechanism of Ni-Catalyzed Coupling of Photoredox Generated Alkyl Radicals and Aryl Bromides: A Computational Study. *Int. J. Mol. Sci.* **2023**, *24*, 9145. (b) Ting, S. I.; Williams, W. L.; Doyle, A. G. Oxidative Addition of Aryl Halides to a Ni(I)-Bipyridine Complex. *J. Am. Chem. Soc.* **2022**, *144*, 5575–5582.

(29) Zuo, Z.; Cong, H.; Li, W.; Choi, J.; Fu, G. C.; MacMillan, D. W. C. Enantioselective Decarboxylative Arylation of α -Amino Acids via the Merger of Photoredox and Nickel Catalysis. *J. Am. Chem. Soc.* **2016**, *138*, 1832–1835.

(30) Beil, S. B.; Chen, T. Q.; Intermaggio, N. E.; MacMillan, D. W. C. Carboxylic Acids as Adaptive Functional Groups in Metal-laphtoredox Catalysis. *Acc. Chem. Res.* **2022**, *55*, 3481–3494.

(31) Zhang, Y.; Tanabe, Y.; Kuriyama, S.; Nishibayashi, Y. Photo-redox- and Nickel-Catalyzed Hydroalkylation of Alkynes with 4-

Alkyl-1,4-dihydropyridines: Ligand-Controlled Regioselectivity. *Chem. Eur. J.* **2022**, *28*, e202200727.

(32) (a) Schely, N. D.; Fu, G. C. Nickel-Catalyzed Negishi Arylations of Propargylic Bromides: A Mechanistic Investigation. *J. Am. Chem. Soc.* **2014**, *136*, 16588–16593. (b) Diccianni, J.; Lin, Q.; Diao, T. Mechanisms of Nickel-Catalyzed Coupling Reactions and Applications in Alkene Functionalization. *Acc. Chem. Res.* **2020**, *53*, 906–919.

